Tabriz Journal of Electrical Engineering (TJEE), vol. 55, no. 1, 2025 Serial no. 111
DOI: 10.22034/tjee.2024.61760.4851

A Novel Method to Estimate Thevenin Equivalent Circuit Using Local Measurements

Pouria Akbarzadeh Aghdam, Hamid Khoshkhoo*

Faculty of Electrical Engineering, Sahand University of Technology, Sahand New Town, Tabriz, Iran
p.akbarzadeh@sut.ac.ir , khoshkhoo@sut.ac.ir

Received:22/04/2024, Revised: 20/08/2024, Accepted 28/09/2024.

Abstract
This paper presents an approach to precisely estimate the Thevenin Equivalent Circuit (TEC) observed from a target bus by utilizing locally measured data. The proposed method relies solely on the voltage magnitude and the power transmitted through the target bus, enabling it to forecast TEC using data provided by WAMS and/or SCADA. Moreover, due to its reliance on local measurements, the proposed method serves as a suitable tool for distributed remedial action schemes to estimate the loadability margin and automatically execute corrective actions, even in the absence of wide-area measured data. Time-domain simulations conducted on Nordic32, IEEE 39-bus, and IEEE 33-bus distribution networks, and the comparison of these results with previously proposed methods in the literature, demonstrate that the proposed algorithm takes into account the system's topology and loading changes and accurately estimates the TEC in both transmission and distribution systems.

Keywords
Thevenin equivalent circuit, Power system analysis, Voltage stability assessment.

1. Introduction

An analysis of power system blackouts over the past decades reveals that voltage instability has emerged as a significant threat to power systems around the world [1]. Moreover, the continuous rise in electrical energy consumers has brought power systems closer to their stability limits, posing a substantial security risk. As a result, several methods have been proposed to promptly assess voltage stability and provide power system operators with the opportunity to implement necessary preventive and corrective measures.

While dynamic simulation-based voltage assessment methods offer accuracy, their high computational burden and the reliance on dynamic data, which may be unavailable in some power systems, have led researchers to explore static methods to estimate the stability boundary. For instance, methods based on PV and QV curves have been proposed in the literature, where system instability is indicated by the divergence of load flow analysis [2], [3]. In addition, some other methods have also been proposed to assess network stability, including dynamic stability assessment [4], [5], the utilization of artificial intelligence [6], [7], Stability indices [] and also stability assessment of EV parking lots in the distribution systems [].

Also, impedance matching condition is used to determine the stability boundary and loadability margin. In such approaches, firstly, the TEC seen from a target bus (e.g., Bus 2 in Fig. 1) is estimated and then, the Thevenin impedance, Z_{th}, is compared to the load impedance, Z_{load} [10]. According to the impedance matching condition, when the target bus reaches its maximum loadability point, $|Z_{th}|=|Z_{load}|$ and the operating point will be at the stability boundary [11], [12].

Obviously, in these methods, accurate calculation of the Thevenin equivalent impedance plays a major role [13], [14]. Therefore, various methods have been proposed in the literature to calculate the equivalent impedance and the Thevenin voltage source seen from the target bus.

Almost, most of the methods which estimate the TEC, use the Single-Port Z-Match method (SPZM), where two successive voltage (V_{load} and V'_{load}) and current (I_{load} and I'_{load}) phasors are measured locally at the target bus and then, TEC seen from that bus is calculated using (1) and (2) [10].

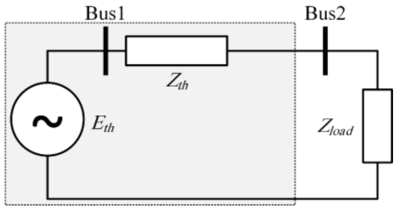

Fig. 1. Thevenin equivalent seen from the receiving bus.

$$\boldsymbol{Z_{th}} = \frac{\boldsymbol{V_{load}} - \boldsymbol{V'_{load}}}{\boldsymbol{I'_{load}} - \boldsymbol{I_{load}}} \tag{1}$$

$$\boldsymbol{E_{th}} = \boldsymbol{Z_{th}}\boldsymbol{I_{load}} + \boldsymbol{V_{load}} \tag{2}$$

Since any changes in the system topology and loading vary TEC parameters and may adversely affect the TEC estimation, Wang et al. have proposed a Coupled Single-Port Circuit (CSPC) based approach to consider the effect of these changes on TEC [15]. Nevertheless, the proposed method requires wide-area measured data provided by WAMS or SCADA and cannot determine TEC using local measurement. Besides, to deal with the dynamic nature of Z_{th} and E_{th} to improve the accuracy of TEC estimation, an improved CSPC method has been proposed in [15] which still requires WAMS and cannot assess the stability using local measurements.

In [16], considering the dynamic behavior of wind turbines, an attempt has been made to calculate the TEC. Also, [17] and [18] have calculated the TEC using the values measured by the PMUs. However, in these research works, the calculation of the network admittance matrix is mandatory and hence, it is necessary to receive the network topology data to calculate the Thevenin equivalent. In [19], a simplified voltage stability analysis method is proposed to use a static TEC. However, in this study, only X_{th} is assumed in the simulations and R_{th} is ignored. Moreover, reference [20] studied about a novel method to estimate the TEC. It is necessary to mention that proposed method in this paper can only calculate the TEC seen from a generator bus and not another busses.

In [21], to calculate E_{th} and X_{th}, an interval for the equivalent reactance is selected. Then, for an arbitrary reactance value, the value of E_{th} is determined. Next, by averaging, calculating the error, and reducing it, the accurate values of E_{th} and X_{th} are obtained. It should be noted that despite the simplicity of this algorithm, it neglects R_{th} and does not calculate the angle of E_{th}.

Besides, [11] has proposed a method to determine TEC using local measurement provided by WAMS with a high sampling rate. Although the method can appropriately determine the stability status, the simulation results presented in Section 4 will show that the actual PV curve of the target bus and the one obtained by this method are somewhat different. Besides, this method requires WAMS and cannot determine TEC using SCADA measurements. In addition, since the method neglects R_{th}, it seems that it cannot determine the Thevenin equivalent parameters in sub-transmission or distribution systems.

In this paper, to overcome problems mentioned above, a new algorithm has been proposed to calculate the TEC. The main advantages of the proposed method are:

- **Low computational burden:**The proposed method has a low computational burden, allowing for rapid assessment of voltage stability and timely implementation of necessary actions.
- **Estimation of TEC using local measurement**: the proposed method accounts for changes in the system's topology and loading, calculating TEC using only data measured at the target bus. Therefore, if there is an unforeseen interruption of the telecommunication system that prevents the transmission of data to or from other parts of the power grid, this method can still calculate the TEC at the target bus. As a result, it serves as a suitable tool for a distributed remedial action scheme.
- **Requiring SCADA and/or WAMS**: to estimate TEC, the proposed method requires voltage magnitude and the power flowing through the target bus. Therefore, unlike the majority of the methods proposed in the literature, this algorithm can estimate TEC using data provided by SCADA and/or WAMS.
- **Applicable in transmission and distribution networks**: Unlike previously proposed methods that can be used in the transmission system, the proposed method estimates both R_{th} and X_{th}. Therefore, it can accurately estimate TEC in both transmission and distribution systems.

In this respect, the outstanding innovation of the proposed algorithm lies in its use of a new mathematical equation to obtain the PV curve for calculating the TEC, in which the Thevenin resistance is accounted for, resulting in a significant increase in accuracy. Additionally, the algorithm operates based solely on local measurements, which, as described above, are of great importance.

In Section 2 of this paper, the relation between the power and voltage of a two-bus network is presented which will be used in Section 3 to propose an appropriate approach to estimate TEC. Then, in Section 4, extensive simulation results on three different networks, i.e., Nordic32, IEEE 39-bus, and IEEE 33-bus distribution systems, have been given that verify the performance of the proposed method in different conditions. Finally, conclusions will be presented in Section 5.

2. Preliminaries

In Fig. 2, neglecting the line resistance (R), the relationship between the voltage and the active power passing through the receiving bus is [22]:

$$v^2 = -(2p\tan\varphi - 1) \pm \frac{\sqrt{(2p\tan\varphi - 1)^2 - 4p^2\sec^2\varphi}}{2} \tag{3}$$

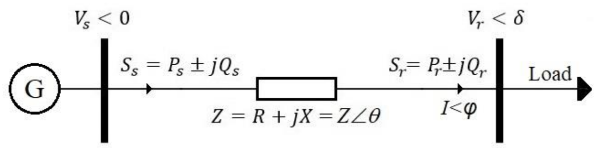

Fig. 2. Two-bus equivalent network.

where v and p are the normalized voltage and active power passing through the receiving bus, respectively, and tan φ depends on the power factor of the load.

In transmission lines, X/R>>1 and hence, in those methods which estimate the TEC, usually R_{th} is neglected. However, it is crucial to note that R_{th} not only depends on lines' resistance, but also on the parameters of other equipment (e.g., loads, transformers, generators, etc.) and cannot be neglected even in transmission systems. Therefore, instead of (3), in this paper the C-PV (Complete PV) curve is used where the resistance R has been considered [23]:

$$v_k^2 = \frac{1 - p_k\sigma \pm \sqrt{1 - 2p_k\sigma - 4\alpha^2 p_k^2}}{2} \;;\; v_k > 0 \tag{4}$$

$$\alpha = \frac{\left({}^{R}/_{X}\right)^2 \tan\varphi - {}^{R}/_{X}}{\left({}^{R}/_{X}\right)^2 + 1} \tag{5}$$

$$\sigma \triangleq \beta + \gamma \tag{6}$$

$$\beta \triangleq 1 + {}^{R}/_{X} \tan\varphi \tag{7}$$

$$\gamma \triangleq \alpha\left(\frac{1 - \left({}^{R}/_{X}\right)^2}{{}^{R}/_{X}}\right) \tag{8}$$

where v_k and p_k are the normalized voltage magnitude and active power passing through the receiving bus (Fig. 2). Also, as mentioned in [23], the C-PV curve which depends on R/X may be rewritten as:

$$k^2v_k^2 = \frac{k^2-(k^2p_k)\sigma \pm \sqrt{k^4(1-2p_k\sigma-4\alpha^2p_k^2)}}{2} \quad (9)$$

Considering $k_1=\sigma/2$, $k_2=\alpha^2$ and $p=k^2p_k=P_r/P_{rB}$, $v=kv_k$ the above equation can be rewritten as:

$$v^2 = {k^2}/{2} - k_1 p \pm \sqrt{{k^4}/{4} - k_1k^2p - k_2p^2} \quad (10)$$

where P_r and P_{rB} are the active power passing through the receiving bus and the base active power, respectively. Also:

$$k = \sqrt{\frac{P_s}{P_{rB}}} = \frac{V_s}{V_{ref}} \quad (11)$$

where V_{ref} is the reference voltage and P_{rB} is calculated as follows:

$$P_{rB} \triangleq \frac{RV_{ref}^2}{R^2+X^2} = \frac{RV_s^2}{k^2(R^2+X^2)} \quad (12)$$

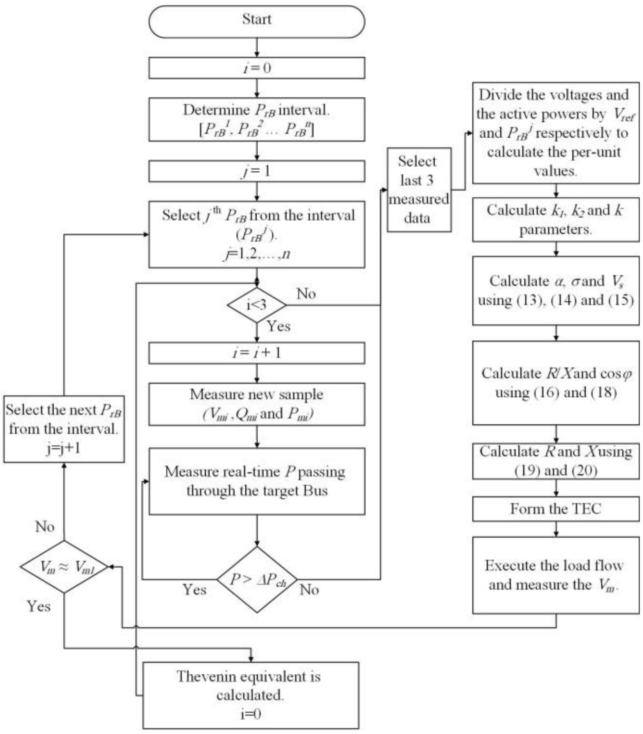

Fig. 3. Flowchart of proposed algorithm to obtain TEC.

3. Proposed algorithm

In this section, based on the C-PV curve, a novel approach has been proposed to determine TEC using local measurements. The flowchart of this approach is shown in Fig. 3 which may be described as follows:

- **Step 1:** Select a target bus as the receiving bus for TEC. It is worth mentioning that while the selected bus does influence the accuracy of the algorithm's results, the differences in accuracy among the various buses are minor. Based on the authors' investigation, it is advisable to choose a bus connected to one or more loads, as this can yield slightly more accurate results.
- **Step 2:** Assign the nominal voltage of the target bus to V_{ref}. Also, consider an arbitrary interval P_{rB}^{range} which will be used in the next steps to determine P_{rB} (in simulations presented in Section 4, $P_{rB}^{range} = 500 \sim 1000\ MW$).
- **Step 3:** At the last three successive operating points (by increasing or decreasing the loading), measure the voltage and the active and reactive powers passing through the target bus: V_{mi}, P_{mi}, and Q_{mi}; i=1,2,3. It is worthwhile noting that in this paper, when the active power passing through the bus changes more than ΔP_{ch} (=1 MW), a new measurement is made. The arrangement of the measurements is shown in Fig. 4.
- **Step 4:** Normalize the measured voltages (V_{m1}, V_{m2}, and V_{m3}) by V_{ref} and calculate the per-unit values. Also, select the minimum value in the interval P_{rB}^{range} and name it P_{rB} . Then, normalized the measured active powers (P_{m1}, P_{m2}, and P_{m3}) by P_{rB}.

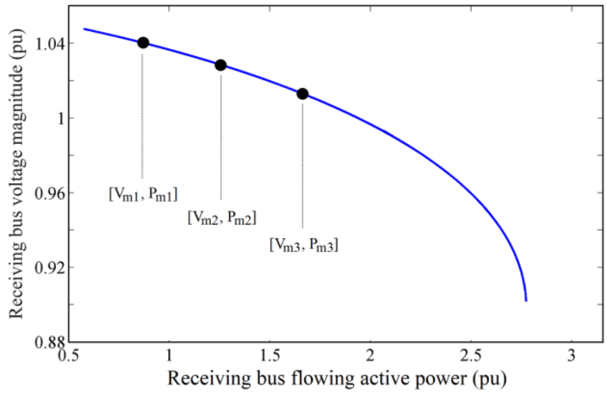

Fig. 4. An example of three sampled operating points.

- **Step 5:** Put the normalized voltages and active powers (obtained in Step 4) in (10) and solve the three equations of three unknowns: k_1, k_2, and k.
- **Step 6:** Calculate α, σ and the sending bus voltage V_s by:

$$\alpha = \sqrt{k_2} \quad (13)$$

$$\sigma = 2k_1 \quad (14)$$

$$V_s = k \times V_{ref} \quad (15)$$

- **Step 7:** Using the following equations derived from (5) and (6), calculate R/X and tan(φ). Then, the power factor can be calculated by (18):

$$R/X = \frac{2\alpha}{\sigma-2} \quad (16)$$

$$tan\,\varphi = \frac{4\alpha^2+\sigma^2-2\sigma}{4\alpha} \quad (17)$$

$$cos\varphi = \frac{1}{\sqrt{1+tan\varphi^2}} \quad (18)$$

- **Step 8:** Based on (16) and (12), calculate the Thevenin impedance, R and X using following equations. As can be seen, R and X depend on P_{rB} which has been selected at Step 4.

$$\boldsymbol{R} = \frac{(\boldsymbol{R}/\boldsymbol{X})^2\, \boldsymbol{V}_{ref}^2}{\boldsymbol{P}_{rB}((\boldsymbol{R}/\boldsymbol{X})^2 + \boldsymbol{1})} \tag{19}$$

$$\boldsymbol{X} = \frac{(\boldsymbol{R}/\boldsymbol{X})\, \boldsymbol{V}_{ref}^2}{\boldsymbol{P}_{rB}((\boldsymbol{R}/\boldsymbol{X})^2 + \boldsymbol{1})} \tag{20}$$

- **Step 9:** Use the calculated parameters (V_s, cos (φ), R, and X) and form the TEC seen from the target bus. Then, in Fig. 2, set the active and reactive power consumption of *Load* to P_{m1}, and Q_{m1}, respectively, execute power flow analysis, and obtain the voltage at the target bus V_m. If V_m is close enough to V_{m1}, the selected P_{rB} is correct. Therefore, stop the procedure and save the Thevenin equivalent parameters (V_s, R, and X in Fig. 2). Otherwise, if $V_m \neq V_{m1}$, the selected P_{rB} is not correct. Thus, increase P_{rB} by ΔP_{rB} and repeat Step 4-Step 9.

It should be noted that in the event of a disturbance causing a change in the network topology, the algorithm's performance may be inaccurate if some samples reflect the pre-disturbance condition while others represent the post-disturbance condition. However, once all three samples are from the post-disturbance condition, the algorithm will provide an accurate response.

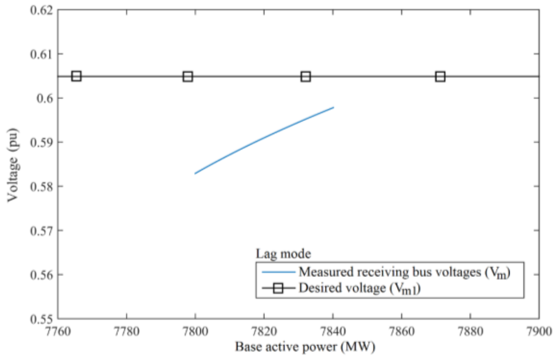

Fig. 5. An example of the voltage matching plot.

According to the proposed method, the determination of P_{rB} is a time-consuming procedure and may result in a high computational burden. To speed up the procedure, in this paper "Voltage matching" plot is used where the voltage at the target bus, V_m (the voltage obtained from power flow analysis mentioned in Step 9), are drawn along with measured voltage V_{m1} (Fig. 5). In this paper, ΔP_{rB} is selected based on the difference between V_m and V_{m1} which significantly decreases the computational burden and speeds up the procedure.

It should be noted that the algorithm presented for calculating the equivalent circuit requires local data. If there is a change in network topology, such as equipment outages or an N-2 condition, the algorithm can be reapplied using new samples. This will produce a revised equivalent circuit that accurately reflects the updated network configuration.

4. Simulation Results

To analyze the proposed method's performance, it has been implemented in Nordic32 [24], IEEE 39-bus [25], and IEEE 33-bus distribution [26] grids and the results have be compared with the performance of the SPZM (Single-Port Z-Match) [10] and LPMA (Local Phasor Measurement Algorithm) [11]. It should be noted that unlike some approaches that use wide-area measured data, SPZM and LPMA use local measurement. Also, mention should be made that both SPZM and LMPA methods need phasor measurements obtained by WAMS (i.e., with a high sampling rate). However, the proposed algorithm can determine TEC using SCADA and/or WAMS measurements.

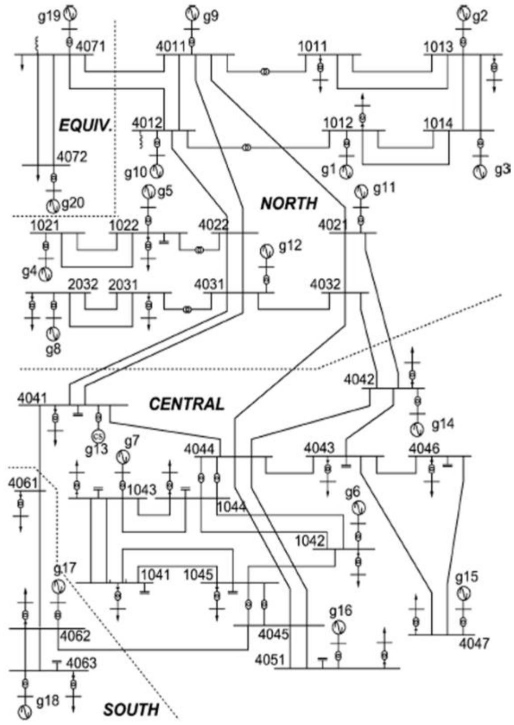

Fig. 6. The Nordic32 test system [22].

In this respect, the DSL environment of DIgSILENT PowerFactory Software is used to model synchronous generators' controllers (automatic voltage controller, governor, and PSS). Also, voltage-dependent loads are modeled to simulate the dynamic behavior of power systems accurately. In these simulations, to check the performance of the proposed method and compare it with SPZM and LPMA, the obtained dynamic results have been used to calculate TECs and to draw the estimated PV curves. Then, these curves will be compared with the actual PV curve of the target bus obtained from the measurement. The better a method's efficiency, the closer the related PV curve will be to the actual PV curve.

4.1. Scenario 1

In this subsection, in the Nordic32 test system shown in Fig. 6, the power consumption of Load1041 is increased. Then, to determine the TEC seen from Bus1041 and the corresponding PV curve, the voltage and the power of Load 1041 are measured and applied to the proposed method.

Fig. 7 shows the actual PV curve of this bus and the PV curves drawn using TEC obtained from the proposed method, SPZM, and LMPA methods. According to these results, the proposed method can estimate TEC and the related PV curve more accurately. Also, Fig. 8 shows the voltage and power passing through some buses.

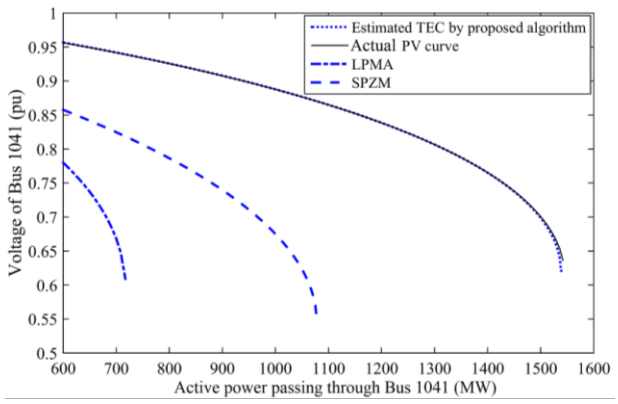

Fig. 7. The estimated and actual PV curves in Scenario 1.

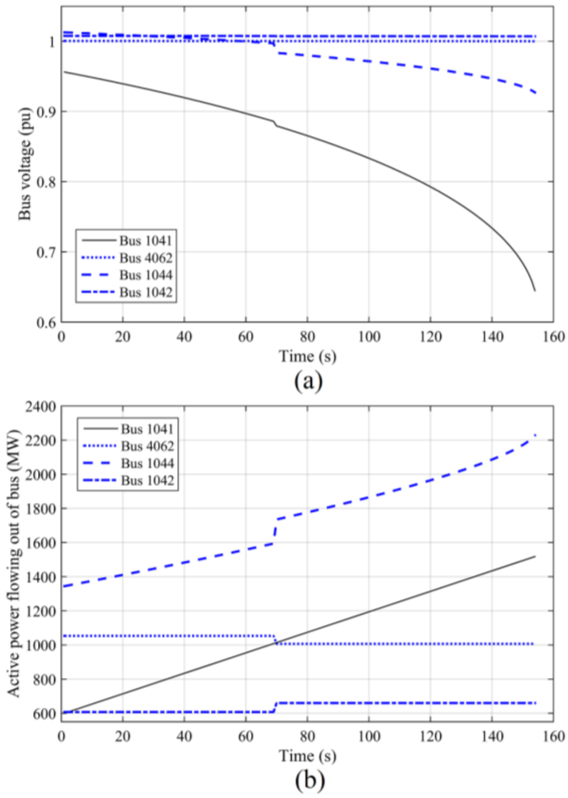

Fig. 8. (a) Voltage and (b) active power in Scenario 1.

4.2. Scenario 2

In this subsection, the power consumption of Load 16 in IEEE 39 Bus test system shown in Fig. 9 increases. Then, to analyze the performance of the proposed method in determining TEC seen from Bus 16, the proposed method uses the voltage and power consumption at Bus 16. The results of the TEC estimation which has been obtained using the voltage and power samples measured at about t=300s are given in Table I. Also, Fig. 10 shows the voltage and power changes during the time-domain simulation and Fig. 11 shows the actual PV curve of Bus 16 as well as the estimated PV curves. According to these results, the proposed method can estimate TEC and the related PV curve more accurately.

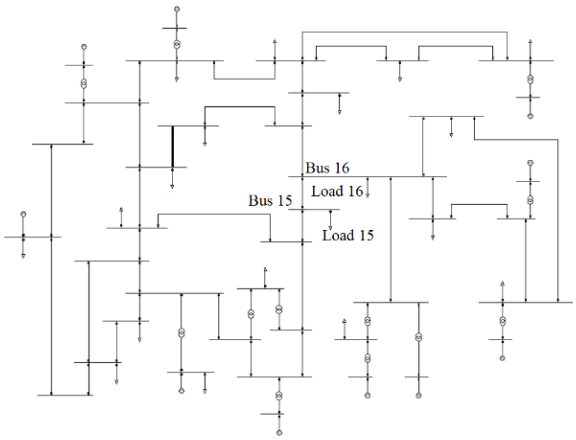

Fig. 9. The IEEE 39 Bus test system.

Table I. The results of TEC in Scenario 2.

V_s (pu)	R (Ω)	X (Ω)	cosφ
1.0732	0.00208848	15.835	0.7955 ind.

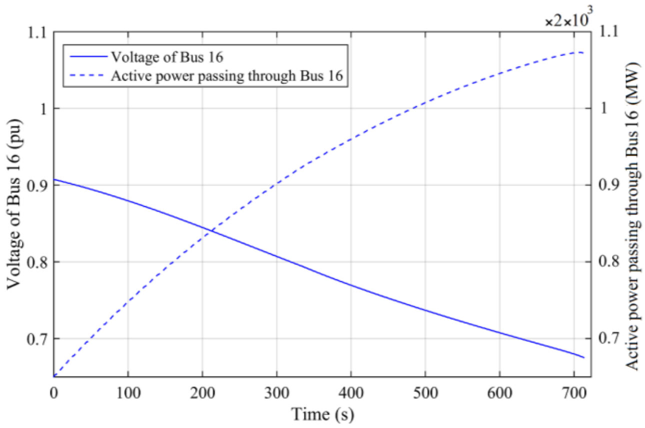

Fig. 10. Voltage and active power passing through Bus 16 in Scenario 2.

4.3. Scenario 3

In this scenario which is simulated on IEEE 39 bus test system, all loads are increasing by 2% every 10 seconds. As shown in Fig. 12, the proposed algorithm has been able to estimate the PV curve with high accuracy.

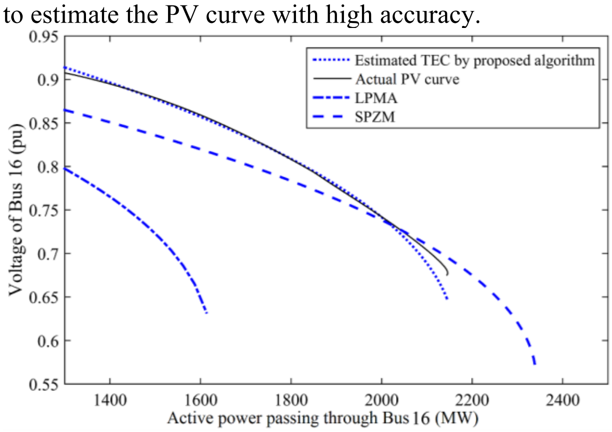

Fig. 11. Estimated PV curves in Scenario 2.

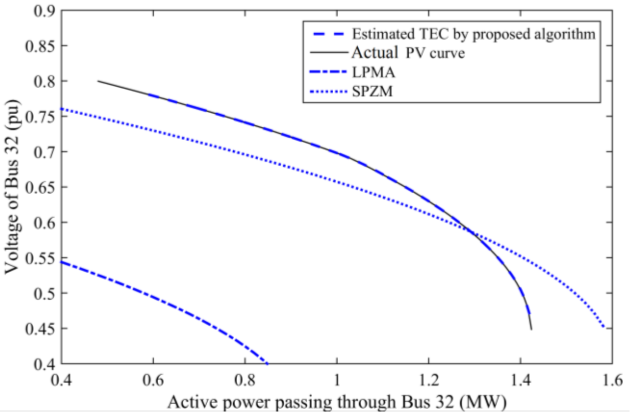

Fig. 12. Estimated PV curves in Scenario 3.

4.4. *Scenario 4*

In this scenario, all loads in IEEE 39-bus test system are increasing by 1% every 10 seconds. Furthermore, when the active power passing through Bus 32 reaches to 1100 MW, a short circuit occurred on the line between Bus 13 and Bus 14 (Line 13-14) causes the system to operate under N-1 condition. As stated in Step 9 of Section 3, in this scenario, the algorithm may initially give an inaccurate response during a short transitional period. However, as shown in Fig. 13, after taking measurements of three samples from the post-disturbance condition, the algorithm's response is highly accurate.

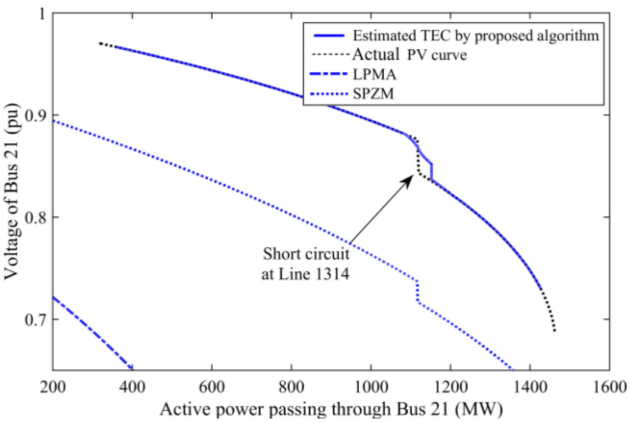

Fig. 13. The actual and estimated PV curves in Scenario 4.

4.5. *Scenario 5*

In this scenario, similar to Scenario 4, all loads of the IEEE 39 bus test system are increasing by 1% every 10 seconds, and when the active power passing through Bus 15 reaches 600 MW, the line between Bus 16 and Bus 17 is disconnected from the network to make a change to the network topology and the PV curve. The comparison of the algorithm's performance with other methods in Fig. 14 confirms that the proposed method accurately estimates the PV curve.

4.6. *Scenario 6*

In this subsection, the methods are implemented on the IEEE 33-bus distribution network (Fig. 15) to analyze the proposed method's performance in a distribution system. In this scenario, the consumption of Load 14 is increased and the measured samples are used to derive the corresponding PV curve.

The actual PV curve of Bus 14 and the estimated PV curves are given in Fig. 16 which indicates that the proposed method can estimate TEC accurately.

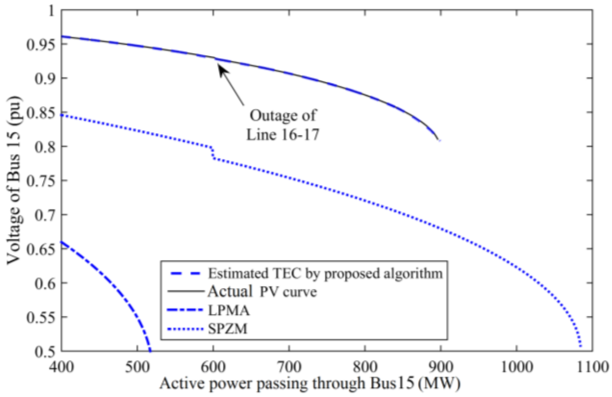

Fig. 14. Estimated PV curves in Scenario 5.

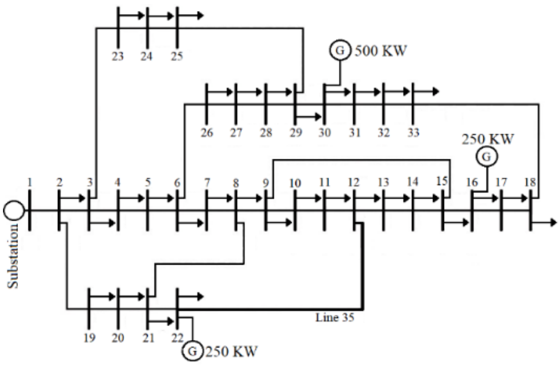

Fig. 15. The IEEE 33 Bus distribution system.

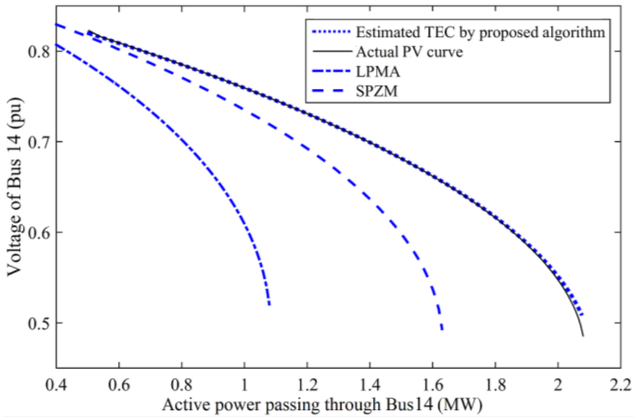

Fig. 16. Obtained PV curves related to Scenario 6.

5. Conclusion

In this research work, a new approach has been proposed which can accurately determine the Thevenin equivalent circuit in transmission and distribution networks using data measured by SCADA and/or WAMS. Even though the proposed method uses locally measured data, the simulation results and the comparison of the proposed method with previous methods proposed in the literature indicate that it can accurately determine the Thevenin equivalent circuit seen from the target bus. Besides, although any changes in the system topology and loading can vary TEC parameters and adversely affect the TEC estimation, these results confirm the performance of this method in such conditions. The simulation results indicate that the accuracy of the proposed algorithm is somewhat influenced by the complexity of the network and the number of devices involved. However, after conducting 50 simulations on the IEEE 39-bus test system, the average accuracy achieved is approximately 95%.

6. References

[1] Eremia, Mircea, M. Shahidehpour, "Handbook of electrical power system dynamics: modeling, stability and control", *John Wiley & Sons*, Vol. 92, 2013.

[2] Guimaraes, Pablo, et al. "QV and PV curves as a planning tool of analysis", In 4th International Conference on Electric Utility Deregulation and Restructuring and Power Technologies (DRPT), 2011.

[3] Almeida, Adriano Batista, "Probabilistic voltage stability assessment considering renewable sources with the help of the PV and QV curves", *IET Renewable Power Generation*, vol. 7, no. 5, pp. 521-530, 2013.

[4] A Khoshkhoo, H., Shahrtash, S, "On-line dynamic voltage instability prediction based on decision tree supported by a wide-area measurement system", *IET Generation, Transmission & Distribution*, vol. 6, no. 11, pp. 1143-1152, 2012.

[5] Khoshkhoo, H., Shahrtash, S, "Fast online dynamic voltage instability prediction and voltage stability classification", *IET Generation, Transmission & Distribution*, vol. 8, no. 5, pp. 957-965, 2014.

[6] A. Parizad, H. Khoshkhoo, S. Dehgan, R. Moradtalab, "An intelligent load and generation shedding procedure in an islanded network using a smart power management system", In International Conferance on Smart Grid Conference (SGC), 2017.

[7] Shahriyari, M., and H. Khoshkhoo, "A Deep Learning-Based Approach for Comprehensive Rotor Angle Stability Assessment", *Journal of Operation and Automation in Power Engineering*, vol. 10, no. 2, pp. 105-112, 2022.

[۸] عباس کارگر، زهرا امینی خوئی، سید یاسر درخشنده، «استفاده از شاخص پایداری ولتاژ P-index برای بهبود پایداری ولتاژ درتقسیم توان راکتیو بین منابع DG در ریز شبکه جزیره‌ای»، مجله مهندسی برق دانشگاه تبریز، ۱۴۰۳.

[۹] محمد جواد جهانی، میثم جعفری نوکندی، حمید اصغری راد، «تخصیص پارکینگ های شارژ خودروهای برقی در شبکه توزیع با در نظر گرفتن پایداری ولتاژ»، مجله مهندسی برق دانشگاه تبریز، ۱۴۰۳.

[10] W Vu, Khoi, "Use of local measurements to estimate voltage-stability margin", *IEEE Transactions on Power Systems*, vol. 14, no. 3, pp. 1029-1035, 1999.

[11] Corsi, Sandro, Glauco N. Taranto, "A real-time voltage instability identification algorithm based on local phasor measurements", *IEEE transactions on power systems*, vol. 23, no. 3, pp. 1271-1279, 2008.

[12] Smon, Ivan, Gregor Verbic, Ferdinand Gubina, "Local voltage-stability index using Tellegen's theorem", *IEEE Transactions on Power Systems*, vol. 21, no. 3, pp. 1267-1275, 2006.

[13] Kroposki, Benjamin, "Achieving a 100% renewable grid: Operating electric power systems with extremely high levels of variable renewable energy", *IEEE Power and Energy Magazine*, vol. 15, no. 2, pp. 61-73, 2017.

[14] Qazi, Atika, "Towards sustainable energy: a systematic review of renewable energy sources, technologies, and public opinions", *IEEE Access* 7, pp. 63837-63851, 2019.

[15] Cui., Bai, Zhaoyu Wang, "Voltage stability assessment based on improved coupled single-port method", *IET Generation, Transmission & Distribution*, vol. 11, no. 10, pp. 2703-2711, 2017.

[16] Chang, Ping, "Research on analytical method of Thevenin equivalent parameters for power system considering wind power", In 12th IEEE PES Asia-Pacific Power and Energy Engineering Conference (APPEEC), IEEE, 2020.

[17] Bidadfar, Ali, Hossein Hooshyar, Luigi Vanfretti, "Dynamic Thévenin equivalent and reduced network models for PMU-based power system voltage stability analysis", *Sustainable Energy, Grids and Networks*, vol. 16, pp. 126-135, 2018.

[18] Yun, Zhihao, Xinhui Cui, Kaigang Ma, "Online thevenin equivalent parameter identification method of large power grids using LU factorization", *IEEE Transactions on Power Systems*, vol. 34, no. 6, pp. 4464-4475, 2019.

[19] Osbouei, B. Alinezhad, and H. Kazemi Karegar. "Estimation of power system Thevenin equivalent based on phasor measurements", *Scientia Iranica. Transaction D, Computer Science & Engineering, Electrical*, vol. 25, no. 6, pp. 3559-3568, 2018.

[20] Burchett, Stephen M., et al. "An optimal Thevenin equivalent estimation method and its application to the voltage stability analysis of a wind hub", *IEEE Transactions on Power Systems*, vol. 33, no. 4, pp. 3644-3652, 2017.

[21] Burchett, Stephen M., "An optimal Thevenin equivalent estimation method and its application to the voltage stability analysis of a wind hub", *IEEE Transactions on Power Systems*, vol. 33, no. 4, pp. 3644-3652, 2017.

[22] Ajjarapu, Venkataramana. "Computational techniques for voltage stability assessment and control", *Springer Science & Business Media*, 2007.

[23] Aghdam, Pouria Akbarzadeh, Hamid Khoshkhoo, "Voltage stability assessment algorithm to predict power system loadability margin", *IET Generation, Transmission & Distribution*, vol. 14, no. 10, pp. 1816-1828, 2020.

[24] Ospina, Luis David Pabón, Andrés Felipe Correa, Gustav Lammert, "Implementation and validation of the Nordic test system in DIgSILENT PowerFactory", *IEEE Manchester PowerTech*, 2017.

[25] Cupelli, Marco, C. Doig Cardet, Antonello Monti, "Voltage stability indices comparison on the IEEE-39 bus system using RTDS", In IEEE International Conference on Power System Technology (POWERCON). IEEE, 2012.

[26] Wazir, Arif, Naeem Arbab, "Analysis and optimization of IEEE 33 bus radial distributed system using optimization algorithm", *Journal of Emerging Trends in Applied Engineering*, vol. 1, no. 2, pp. 17-21, 2016.